

Title:

FEMTOSECOND EXCITED-STATE ABSORPTION
DYNAMICS AND OPTICAL LIMITING IN FULLERENE
SOLUTIONS, SOL-GEL GLASSES, AND THIN FILMS

RECEIVED
SEP 23 1996
OSTI

Author(s):

D. McBranch, V. Klimov, L. Smilowitz, M. Grigorova,
J. M. Robinson, A. Koskelo, and B. R. Matthes
Chemical Sciences and Technology Division, Los
Alamos National Laboratory, Los Alamos, NM 87545

Submitted to:

SPIE proceedings, "Fullerenes and Photonics III", August
4-9, 1996, Denver, CO

MASTER



Los Alamos
NATIONAL LABORATORY

Los Alamos National Laboratory, an affirmative action/equal opportunity employer, is operated by the University of California for the U.S. Department of Energy under contract W-7405-ENG-36. By acceptance of this article, the publisher recognizes that the U.S. Government retains a nonexclusive, royalty-free license to publish or reproduce the published form of this contribution, or to allow others to do so, for U.S. Government purposes. The Los Alamos National Laboratory requests that the publisher identify this article as work performed under the auspices of the U.S. Department of Energy.

Form No. 836 R5
ST 2629 10/91

DISTRIBUTION OF THIS DOCUMENT IS UNLIMITED

44

DISCLAIMER

**Portions of this document may be illegible
in electronic image products. Images are
produced from the best available original
document.**

Femtosecond excited-state absorption dynamics and optical limiting in fullerene solutions, sol-gel glasses, and thin films

D. McBranch, V. Klimov, L. Smilowitz, M. Grigorova,
J. M. Robinson, A. Koskelo, and B. R. Mattes

Chemical Science and Technology Division
Los Alamos National Laboratory, Los Alamos, NM 87545

H. Wang and F. Wudl

University of California, Santa Barbara, CA 93106

ABSTRACT

We compare detailed dynamics of the excited-state absorption for C_{60} in solution, thin films, and entrapped in an inorganic sol-gel glass matrix. Our results demonstrate that the microscopic morphology of the C_{60} molecule plays a crucial role in determining the relaxation dynamics. This is a key factor for applications in optical limiting for nanosecond pulses using reverse saturable absorption. We find that the dynamics of the C_{60} -glass composite occur on long (ns) timescales, comparable to that in solution; thin film samples, by contrast, show rapid decay (<20 picoseconds). These results demonstrate that the C_{60} -sol-gel glass composites contain C_{60} in a molecular dispersion, and are suitable candidates for solid-state optical limiting. Multispectral analysis of the decay dynamics in solution allows accurate determination of both the intersystem crossing time (600 ± 100 ps) and the relative strengths of the singlet and triplet excited-state cross sections as a function of wavelength from 450-950 nm. The triplet excited-state cross section is greater than that for the singlet excited-state over the range from 620-810 nm.

1 INTRODUCTION

Recently, many studies have emerged on optical power limiting (OL) in buckminsterfullerene (C_{60}).¹⁻⁶ OL occurs when the absolute transmittance of a material decreases with increasing laser fluence; in C_{60} , the dominant mechanism for OL is reverse saturable absorption (RSA), in which the absorption cross section from excited-state electronic energy levels is significantly higher than the ground state absorption cross section.² For limiting of nanosecond pulses, the lifetime of the excited-state responsible for the nonlinear absorption is a crucial parameter. In this work, we provide a detailed study of the relaxation dynamics of the excited-state absorption for C_{60} in toluene solution, as a thin solid film, and entrapped within an inorganic sol-gel glass matrix. Our results demonstrate that the microscopic morphology of the C_{60} molecules plays a crucial role in determining the relaxation dynamics. We find that the dynamics in C_{60} -glass composites occur on long (ns) timescales, comparable to those in solution; thin film samples, by contrast, show rapid decay (<20 picoseconds). Combined with intensity-dependent transmission measurements on the same samples, these results demonstrate that the C_{60} /sol-gel glass composites contain C_{60} in a molecular

dispersion, and are suitable candidates for solid-state optical limiting. Despite similarities in dynamics between the sol-gel/fullerene composites and solutions, reduced optical limiting effectiveness is seen in the glass composites. Implications of this reduction will be discussed in light of recent predictions of enhanced nonlinear performance in "bottleneck optical limiters," in which the concentration of nonlinear absorbers is varied along the depth of the sample in conjunction with a tightly-focused laser beam.^{7,8} The extremely high optical damage threshold observed in our gels may allow significantly higher dynamic ranges than those allowed by either solutions or solid polymer/fullerene blends.

Sol-gel techniques provide a means of synthesizing optical quality glasses which include organic optically-active species at reduced temperatures compared to conventional melt processing.⁹ It has been previously demonstrated that fullerenes (including C₆₀,^{6,10,11} C₇₀,¹² and C₆₀ derivatives¹³) can be incorporated into glasses by these methods. These composite materials combine the benefits of a high damage threshold inorganic oxide glass host with the desired optical nonlinearities of the guest species. With the proper processing protocols, composite gels can be formed into monoliths, fibers, or films. Here, we present detailed synthetic procedures for the formation of clear doped glasses using both C₆₀ and the methanofullerenes phenyl-C₆₁-butyric acid cholesteryl ester (PCBCR) and 1-(3-methoxycarbonyl)propyl)-1-phenyl-[6,6]-C₆₁(PCBM).¹⁴ The use of highly soluble derivatives allows the formation of composite glasses over a very wide range of fullerene concentrations.

2 EXPERIMENTAL

The starting solution for the sol-gel synthesis (precursor sol) was prepared from mixtures of two solutions (A and B) in the following manner. Solution A consisted of 11 ml tetramethyl orthosilicate (TMOS) (11.25 g, 0.0739 mol) and 5 ml deionized water (4.96 g, 0.275 mol). Solution B consisted of 30 ml tetraethyl orthosilicate (TEOS) (28.02 g, 0.134 mol), 7.5 ml deionized water (7.51 g, 0.691 mol), and 11 ml TMOS (11.25 g, 0.0739 mol). Both solutions were sonicated for 15 min. Two drops of 38% HCl were added to A which resulted in a highly exothermic hydrolysis reaction, and both solutions were sonicated for an additional 15 min. Solution A was added dropwise to solution B, resulting in a clear monophasic sol. The combined molar ratio of TEOS:TMOS:H₂O was 1:1.1:5.3.

Undoped porous glass samples were then prepared, in which 1, 2, or 3 ml of either toluene or o-dichlorobenzene (DCB) was added to each vial containing 7 ml of sol. The sol and co-solvent mixtures were mechanically stirred to ensure homogeneity. Either 1.0 or 0.5 ml portions of the toluene-sol and dichlorobenzene-sol mixtures were pipetted into PTFE containers. DCB samples were placed into an oven at 60 °C. Gelation was observed in 1-3 hours after sol formation. Toluene samples were cured either at room temperature or at 40 °C. The gelation point was reached in 1-3 hours for oven cured samples, and in 8-10 hours for room temperature samples.

Silica gels containing C₆₀, PCBCR, and PCBM were prepared using this precursor sol as a starting point. For C₆₀, both toluene and dichlorobenzene were used to prepare 2.5 mg/ml solutions. Rather than simply mixing the precursor sol and fullerene solutions, it was found to be necessary to first mix small amounts of solvent into the precursor sol, in order to achieve monophasic solutions from which the C₆₀ did not precipitate prior to gelation.^{6,11} The only exception to this was when using DCB as solvent in relatively high amounts. Three different compositions were prepared using toluene solutions, varying the content of C₆₀ in the mixture of precursor sol/carrier solvent/C₆₀ solution. Actual proportions for those compositions were 7 ml of precursor sol to 1, 2, or 3 ml of toluene carrier solvent and 0.1 ml of the C₆₀ solution in toluene. Samples were cured as described above. Resultant samples were clear glasses of light beige color.

Two groups of compositions were prepared with DCB solution: 1) with carrier DCB - 7:0.5:0.5; 7:1:1; 7:1.5:1.5; and 2) without carrier DCB - 7:2; 7:2.5; 7:3; 7:3.5; 7:4; and 7:4.5. For example, composition 7:1:1 contained 7 ml of silicon sol; 1 ml of precursor DCB, and 1 ml of fullerene solution. Upon addition of the purple C₆₀ solution to the sol, a milky brown solution was formed. Either 1.0 or 0.5 ml were pipetted into PTFE containers and aged as described above. All of the initial C₆₀/DCB gels had light to very dark purple color. Samples with the total amount of DCB not exceeding 2.5-3 ml withstood heat treatment up to 180 °C (near the boiling point of DCB), whereas those with

higher DCB content tended to crack and turn opaque. The temperature was raised 25 °C approximately every hour, and then gels were left at 180 °C for at least 8 hours. Quartz self-sealing crucibles (Fisher Scientific) were used for the treatment. Samples turned from purple to brownish-amber upon drying, but kept their clarity and integrity.

DCB was also used to prepare 4.0 mg/ml solutions of PCBCR, and PCBM solutions in the range from 0.896 to 31.13 mg/ml. Compositions were prepared similar to those described above. PCBCR and PCBM form dark brown solutions in DCB; PCBCR/DCB solutions, when mixed with the precursor sol, turn milky. By contrast, PCBM/DCB/precursor sol mixtures form casting solutions that are clear, and have practically the same color as DCB solution. Casting solutions were pipetted into PTFE containers and cured as described above. Upon drying, the color of the PCBCR and PCBM gels did not change, and their clarity and integrity was maintained. The final PCBCR- and PCBM-doped gels had light to very dark yellowish-amber color. After the sol-gels were heat-treated for the removal of the residual solvent, they were found to have sufficient mechanical rigidity to withstand optical polishing and shaping. Samples were polished first with 9 μm aluminum oxide and then with 3 μm silicon carbide (both moistened with silicon oil) to obtain optical quality surfaces. In addition to allowing the concentration of the fullerene guest to be controlled over a wide range, the use of soluble C_{60} derivatives leads to a much higher success rate for forming clear, uncracked monoliths, greater mechanical strength, and greater ability to withstand heat treatment. The most consistent and successful results were obtained using PCBM, for which the methoxy terminating group likely assists in mediating the insolubility of the extremely nonpolar C_{60} in the polar solvents (water, ethanol and methanol) present during the initial mixing and subsequent gelation. This is similar to behavior recently reported using fullerene derivatives terminated with silicon alkoxide groups.¹³

Time-resolved excited-state absorption spectra were measured using a femtosecond (fs) pump-probe technique. The samples were excited at 405 nm by 100 fs pulses from a frequency-doubled regeneratively amplified modelocked Ti:Sapphire laser (Clark-MXR CPA-1000). The pump pulse energy was 5 μJ , corresponding to an excitation density of 12 mJ/cm^2 , and the repetition rate was 1 kHz. Femtosecond white light pulses were generated in a 1 mm sapphire window. The transmission of the sample was measured using a 0.15 m spectrometer and CCD array with the pump beam on (T_{on}) and off (T_{off}), and the differential transmission $\Delta T/T$ was determined from the expression: $\Delta T/T = (T_{on} - T_{off})/T_{off}$. Each spectrum was the average of 500-1000 pulses. Alternately, single wavelength dynamics were monitored with much higher sensitivity by mechanically chopping the pump beam, and using a balanced reference beam and signal beam with differential amplification, followed by lock-in detection. C_{60} samples were prepared in toluene solution in 2 mm path length cells, with concentration adjusted to yield optical density approximately 1 at the pump wavelength. Thin films were prepared by vacuum sublimation, and no attempt was made to preserve them from exposure to oxygen.

Optical limiting in the spectral region from 532-700 nm is measured using a frequency-doubled Nd:YAG laser (Quanta Ray GCR-3 with 6 ns pulses at 532 nm), and pulsed dye laser (Quanta Ray PDL-3 with 5.5 ns pulses from 560-700 nm). Intensity-dependent transmission is determined by placing the sample at the focus of a 100mm (red) or 150mm (green) focal length lens. The beam is split into a reference arm, a sample arm, and an intensity measurement arm with reference and sample transmissions monitored by 13 mm^2 Si photodiodes followed by gated integration. Each point is the average of 25 to 50 laser shots with signal and reference channels normalized shot by shot. The laser intensity is ramped up and down to check for hysteresis due to sample damage or slow heating processes.

3 RESULTS AND DISCUSSION

Our previous measurements in C_{60} solutions^{15,16} performed in the spectral range 550-1100 nm indicated that at short delay times (Δt) between pump and probe pulses the excited state absorption is dominated by a broad band at 975 nm (ω_{S1}). The decay of this band is accompanied by the complementary growth of a new band around 750 nm (ω_{T1}). These dynamics have been explained in terms of singlet-triplet intersystem crossing with a time constant ranging from 650 ps to 1.2 ns.^{15,17,18} The bands ω_{S1} and ω_{T1} were assigned to the excited-state absorptions associated with the lowest excited singlet and triplet states, respectively. In the present experiments we have extended

the transient absorption (TA) measurements down to a probe wavelength of 400 nm, and performed careful studies of single wavelength TA dynamics in the range from 450 to 920 nm.

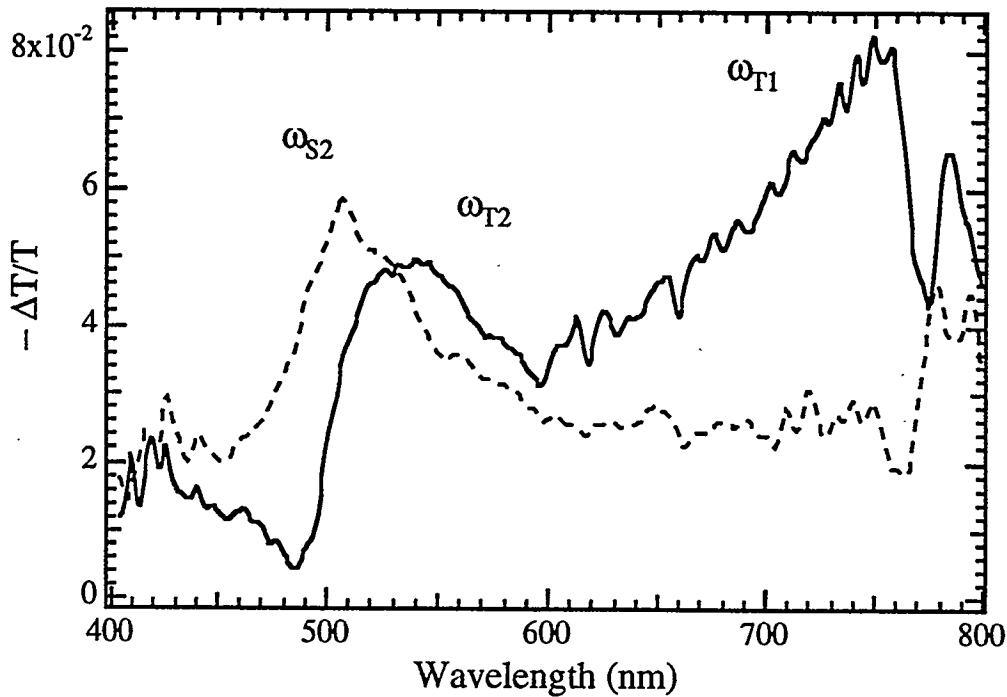


Figure 1. $-\Delta T/T$ spectrum for C_{60} in toluene solution, taken at two delay times: 10 ps (dashed line, singlet excited-state absorption) and 1 ns (solid line, triplet excited-state absorption).

Fig. 1 shows the short wavelength portions of TA spectra measured at 10 ps (dashed line) and 1 ns (solid line) after excitation. In addition to the long wavelength features reported previously,^{15,16} these spectra exhibit two new bands at 500 nm ($\Delta t = 10$ ps) and 530 nm ($\Delta t = 1$ ns) which can be assigned to singlet and triplet excited-state absorption, respectively. This shows that the excited-state absorption contains contributions from at least two different transitions for both the singlet and triplet manifolds. The energies of these transitions are $\sim 1.3\text{--}1.4$ eV (ω_{S1}) and 2.5 eV (ω_{S2}) (singlet absorption), and 1.65 (ω_{T1}) and 2.34 eV (ω_{T2}) (triplet absorption).

To study the intersystem crossing dynamics in more detail, we performed measurements of the TA dynamics in the first 1.0 ns for several wavelengths in the spectral range from 450–920 nm (Fig. 2). Depending on the spectral energy, the transient $\Delta T/T$ curves show either growth or decay, corresponding to a dominant contribution from either the triplet or singlet excited-state, respectively. In particular, we observed a decreasing signal in two separated spectral regions (450–550 nm and 820–920 nm), consistent with early-time TA spectra exhibiting two bands attributed to singlet excited-state absorption.

Previous studies showed that in isolated C_{60} molecules, intersystem crossing occurs with quantum yield 0.96.¹⁹ Under these conditions, the long-term TA dynamics are single exponential with one time constant τ accounting for both the decay of the singlet and growth of the triplet features over the whole spectral range. Introducing the wavelength-dependent excited-state absorption cross sections $\sigma_S(\lambda)$ (singlet) and $\sigma_T(\lambda)$ (triplet) we can model these dynamics as follows:

$$\begin{aligned} -\Delta T/T(\lambda, t) &= n_0[\sigma_S(\lambda)e^{-t/\tau} + \sigma_T(\lambda)(1 - e^{-t/\tau})] \\ &= n_0\sigma_T(\lambda)\left(1 - \frac{\sigma_T(\lambda) - \sigma_S(\lambda)}{\sigma_T(\lambda)}e^{-t/\tau}\right), \end{aligned} \quad (1)$$

where n_0 is the concentration of C_{60} molecules. The TA dynamics can be fit to equation 1 using a single constant $\tau = 600 \pm 100$ ps for all eleven wavelengths measured (Fig. 2). This intersystem crossing time is in agreement with

single-wavelength measurements in Ref. 5. Other authors have determined values for τ as high as 1.2 ns.¹⁸ This work represents to our knowledge the first fit of multiple (eleven) wavelengths to a single time constant, and hence the results are expected to be more definitive than single wavelength fits. These results should establish a firm number for τ , which until now has been in some dispute. In addition to the intersystem crossing time constant, the fitting procedure yields the spectral distribution of the ratio σ_T/σ_S , which is plotted in Fig. 3. According to these data, $\sigma_T > \sigma_S$ in the range 620–810 nm; for wavelengths in this range, optical limiting will be stronger for ns laser pulses than for ps pulses, while outside this range the limiting will be stronger for ps pulses.

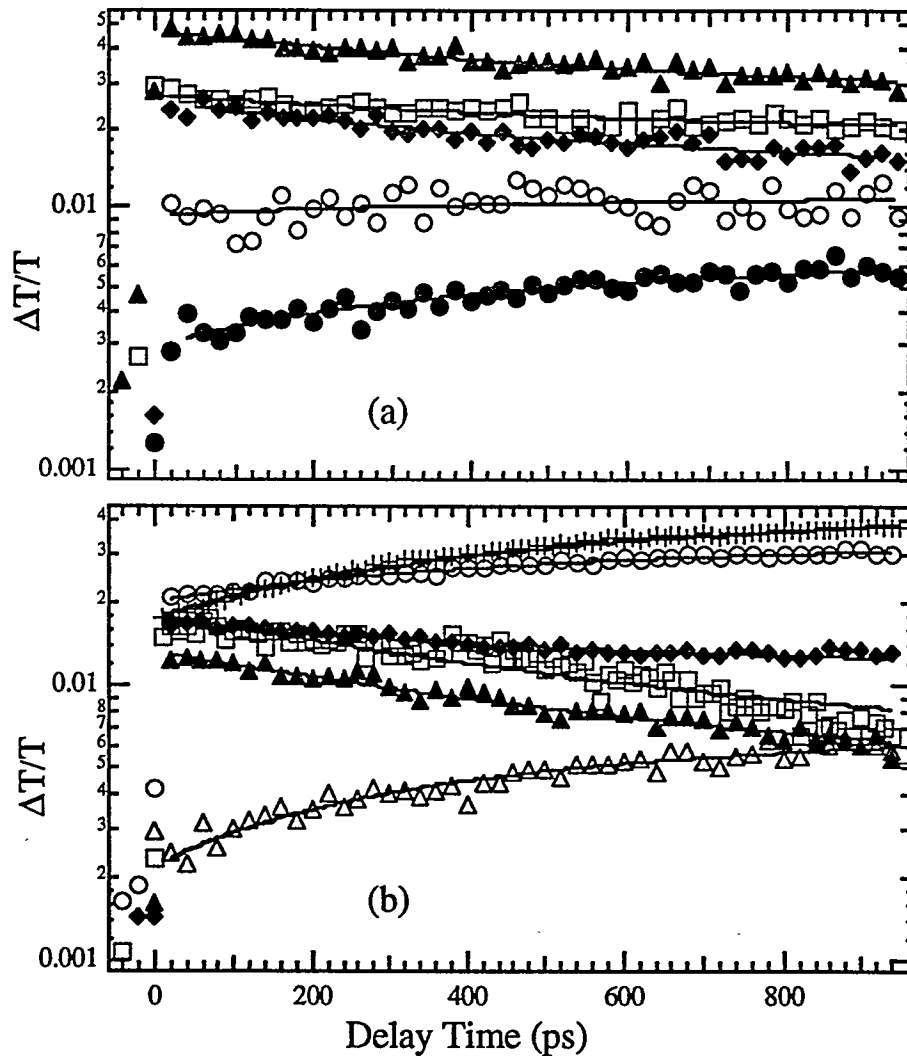


Figure 2. $-\Delta T/T$ vs delay time up to one ns for C_{60} in toluene solution, taken at eleven wavelengths: (a) 450 nm (open squares), 500 nm (solid triangles), 550 nm (solid diamonds), 650 nm (open circles), and 700 nm (solid circles); (b) 725 nm (open triangles), 750 nm (crosses), 780 nm (open circles), 820 nm (solid diamonds), 890 nm (solid triangles), and 920 nm (open triangles). Fits are plotted as solid lines (see text).

In addition to these long-scan measurements, TA dynamics were monitored on much shorter timescales. Fig. 4 plots the short-time dynamics, along with the pump-probe cross-correlation function recorded using the instantaneous two-photon absorption in ZnS. Except for weak features seen at $\Delta t = 0$ (pump and probe pulses overlap inside the sample), the transients for all spectral energies in the range 450–920 nm have almost the same build-up dynamics.

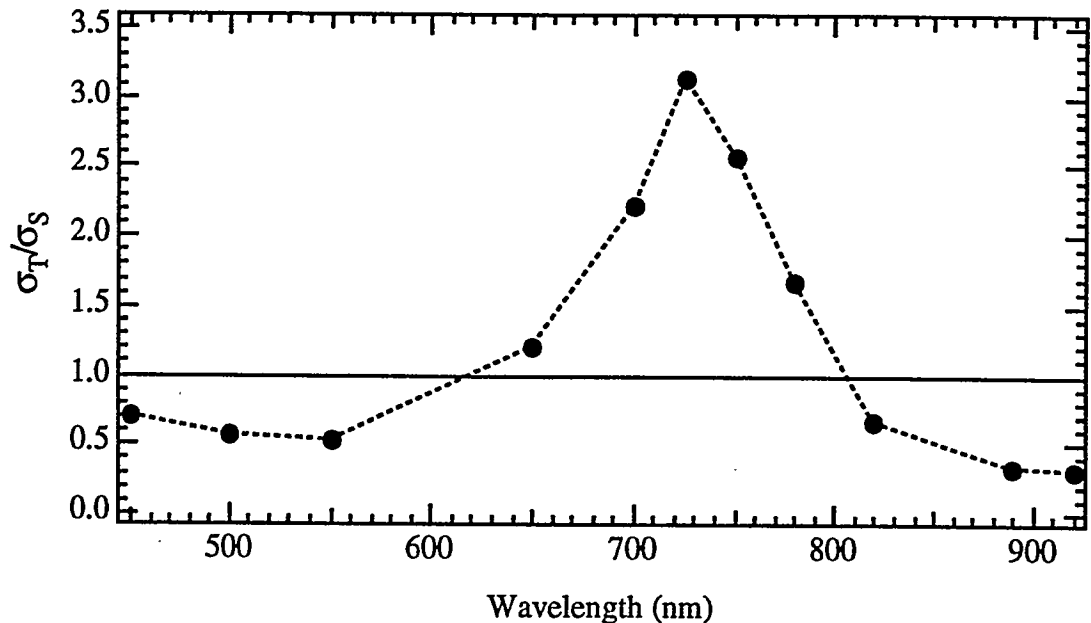


Figure 3. $\frac{\sigma_T}{\sigma_S}$ deduced from fitting dynamics data of Fig. 2 (see text).

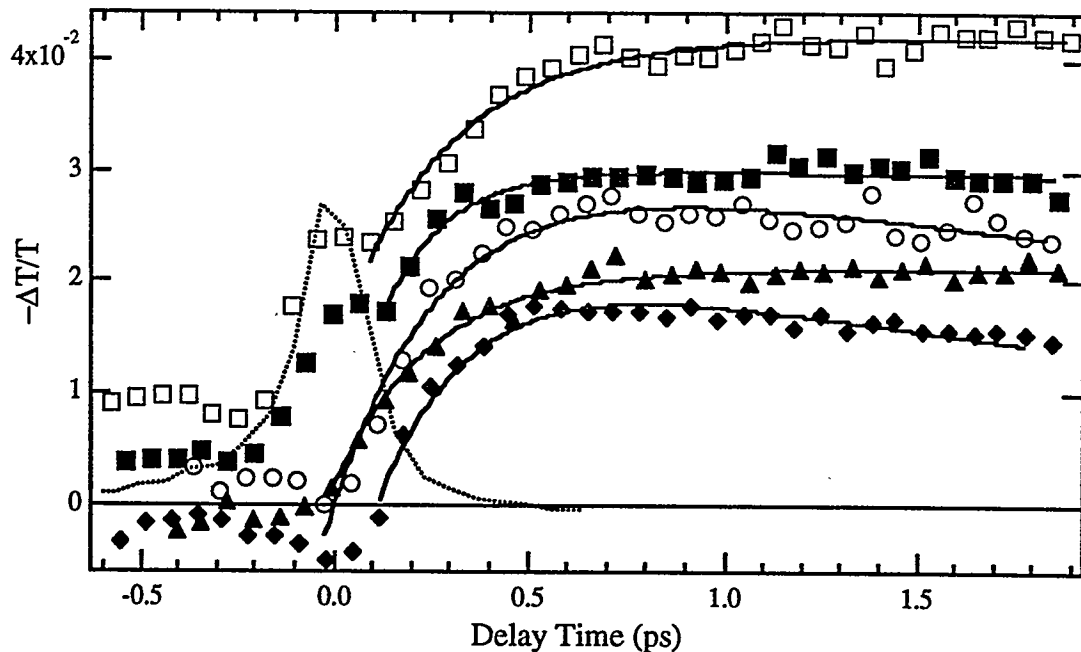


Figure 4. $-\Delta T/T$ vs delay time up to 2 ps for C_{60} in toluene solution, for five wavelengths: (a) 450 nm (open squares), 550 nm (solid squares), 750 nm (open circles), 820 nm (solid triangles), and 920 nm (solid diamonds). Pump/probe cross-correlation is included for reference (dotted line).

Fitting to an exponential growth yields time constants of 200–300 fs. The fast bleaching seen at 450 nm and 550 nm at $\Delta t = 0$ is likely attributed to the pump-induced bleaching of the ground-state absorption, which is quickly overwhelmed by the increased absorption associated with the lowest excited singlet state. The resolution-limited fast increased absorption seen at 750 and 820 nm can be attributed to a two photon absorption process which involves one photon from the pump pulse and the other photon from the probe pulse. This fast response serves to calibrate the

absolute arrival time of the probe pulse relative to the pump, and shows unequivocally that the subsequent growth dynamics involves relaxation from the initially excited state to the lowest excited singlet state.

The TA build-up dynamics are determined by the nature of the initial photoexcitations. The energies of the first (S_1) and second (S_2) excited singlet states in C_{60} are close to 2.5 and 4 eV, respectively.²⁰ Given the energy of the pump photon (3.1 eV), we can conclude that the initial photoexcitations under our experimental conditions are high lying states within the S_1 -vibronic manifold. The energy-redistribution process within this manifold is manifested in the build-up of increased absorption. Due to the large density of vibronic states, this process can be very fast (from subps-to-ps time scales) in large polyatomic molecules.²¹ The 200–300 fs constant derived above provides a measure of the energy redistribution rate within the S_1 -vibronic manifold in C_{60} molecules in solution. Such rapid internal conversion has been proposed as essential to explain both the significant optical limiting for ps pulses,³ and the intensity-dependent recombination in C_{60} thin films.²²

Since for many applications of optical limiters, solid-state samples are desirable, these data for C_{60} solutions are compared in the following to dynamics data for C_{60} thin films, and C_{60} -sol-gel glass composites. In strong contrast to the relaxation dynamics in solution, the dynamics in thin films of C_{60} show a very rapid nonexponential decay on subpicosecond to ps timescales (Fig. 5). The rapid and nonlinear recombination dynamics for C_{60} thin films at high fluences has been attributed to bimolecular recombination due to exciton-exciton annihilation.²² Hence, for ns pulses, the excited-state absorption remains large in solution over a broad wavelength range for the duration of the pulse, while the decay back to the ground-state in the solid thin film is much more rapid than the pulselength. Consequently, RSA on the nanosecond time scale is not observed in the thin film. This is confirmed by intensity-dependent transmission measurements of C_{60} films using ns pulses, in which optical limiting is not observed.¹⁵

The optical absorption in the doped silica sol-gel glasses is broadened relative to that of the fullerenes in solution, and the samples are brown (similar in color to the thin film). The excited-state absorption peaks are also broadened, with no distinct singlet or triplet features, in contrast to the spectra in solution. The strongest evidence that the fullerenes are dispersed in the glass on a molecular scale comes from the relaxation dynamics, which resemble much more closely the solution results than those in thin films. The fact that no increase is observed in Fig. 5b for the magnitude of the excited-state absorption at 750 nm for the C_{60} -doped sol-gel glass (associated with the growth of triplet population) is attributed to the broadening of the excited-state absorption peaks in the glass, so that there is a relatively larger contribution from the singlet at this wavelength. This is due to inhomogeneous broadening from the variable local environment seen by individual C_{60} molecules in the solid state, and is similar to the inhomogeneous broadening seen in the thin film. However, the dynamics show clearly that the C_{60} molecules in the composite glass are well separated compared with the polycrystalline thin films. The results also confirm that the primary mechanism for rapid relaxation in the thin films is the close proximity of adjacent fullerenes, not additional nonradiative relaxation pathways introduced by the disordered solid-state.

Additional insight into the differences between the three samples can be gleaned from a closer examination of the initial growth dynamics of the photoinduced absorption. As seen in Fig. 4, the growth of the singlet excited-state feature in solution is easily resolved within our time-resolution, with a time constant of ≈ 250 fs, independent of wavelength over the range measured. As in the case of the decay dynamics, the thin solid film data in Fig. 5a show substantially faster (resolution-limited) growth dynamics, indicating that the initial relaxation to form the lowest singlet excited state is much more rapid in the thin film than in solution. Presumably, this increased rate arises due to the additional pathways due to hopping to adjacent molecules, with a correspondingly larger density of intermediate vibrational states to facilitate the rapid internal conversion. Again, this is not purely a solid-state effect, since the growth dynamics in the sol-gel glass more closely resembles that in solution than that in the film. Hence, as in the case of the decay, the rapid growth dynamics arises primarily due the proximity of other fullerene molecules.

Previously, it was difficult to perform quantitative comparisons of the optical limiting effectiveness for fullerenes in solution and in the sol-gel composite glasses, since the latter samples are characterized a relatively large amount of linear scattering.⁶ Hence, it is impossible to calibrate the true low intensity transmission in the porous glasses without additional processing. The development of optimized procedures for curing of the fullerene-doped glasses, as detailed above, however, allows a series of glasses to be developed with controlled concentration, high clarity, and sufficient mechanical strength to allow polishing to flat, optical quality surfaces. We have now performed a

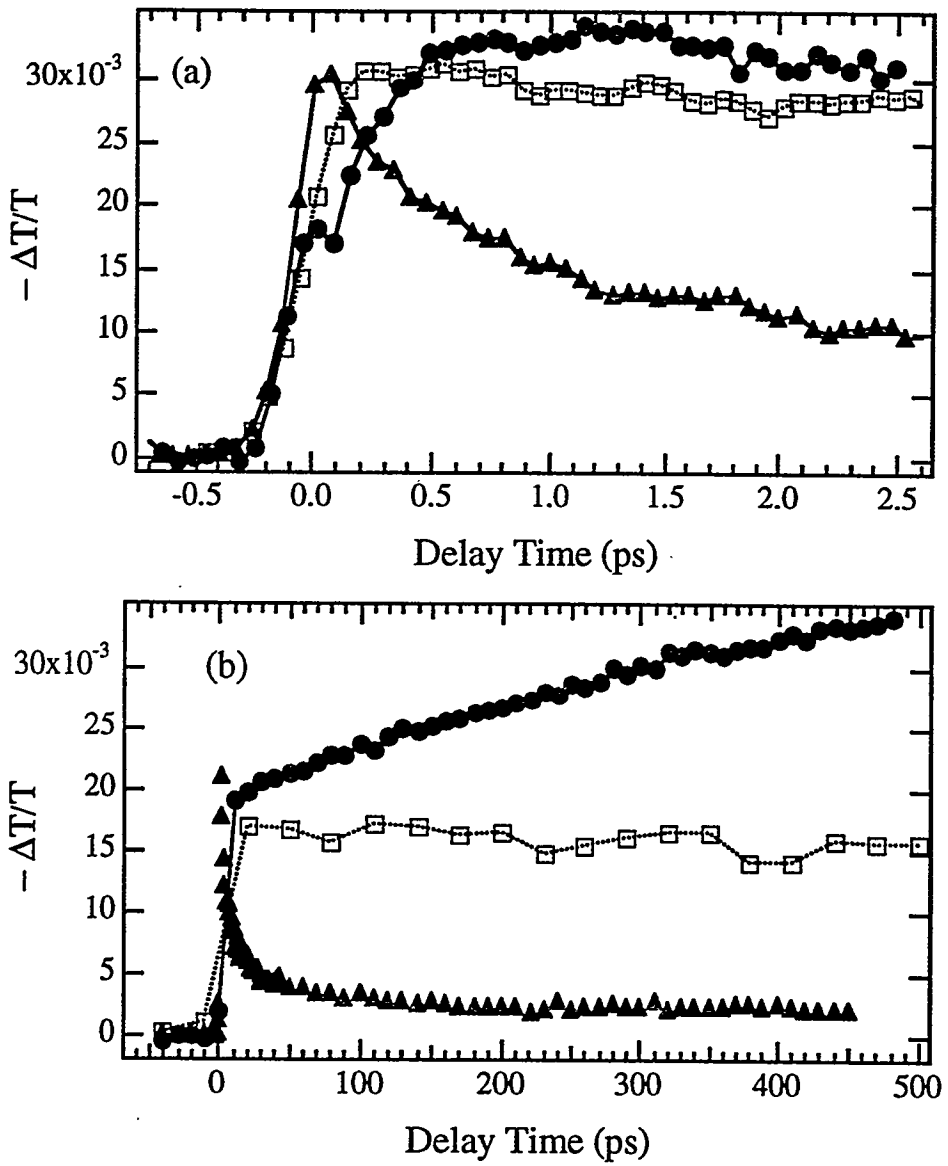


Figure 5. $-\Delta T/T$ at 750 nm vs delay time (a) up to two ps, and (b) up to one ns, for C_{60} in toluene solution (solid circles), in sol-gel glass (open squares), and in thin films (solid triangles).

side-by-side comparison of the optical limiting at 700 nm using $f/15$ focusing optics, as shown in Fig. 6 for a 1 mm cuvette of PCBM/DCB and a 1.2 mm polished PCBM/sol-gel monolith with the same initial transmission ($\approx 70\%$). It is evident from this figure that the transmission at an incident energy of 3 mJ is more than a factor of two lower for the solution than for the sol-gel sample. This is consistent with previous measurements performed using PMMA as a solid-state host for C_{60} , at a wavelength of 532 nm.²³ The primary reason for the difference is that efficient thermal mechanisms which operate at high fluences for ns pulses in solution cannot contribute in the glass composite. However, a significant difference from previous results is that in the glass composite, the damage threshold is 1-2 orders of magnitude higher than that for fullerenes in PMMA. In Fig. 6, the data for solution stops at 3.5 mJ due to damage at the front surface of the cuvette, discernible as a point where the fullerenes precipitate out to form a spot on the surface, with hysteresis in the optical limiting curve upon returning to lower pulse energies. At higher pulse energies, absorption at this spot leads to catastrophic ablative damage of the cell wall. This mechanism is absent in

the glass, however, and no evidence for optical damage was seen at the highest pulse energies available at 700 nm. In fact, we have observed that the damage threshold in solution drops as the fullerene concentration is increased, due to the precipitation effects; in the glass composites, by contrast, the damage threshold (at 532 nm) increases for increasing concentration, since the nonlinear absorption prior to the beam focus acts to protect the sample at the focus at high concentrations and input fluences.

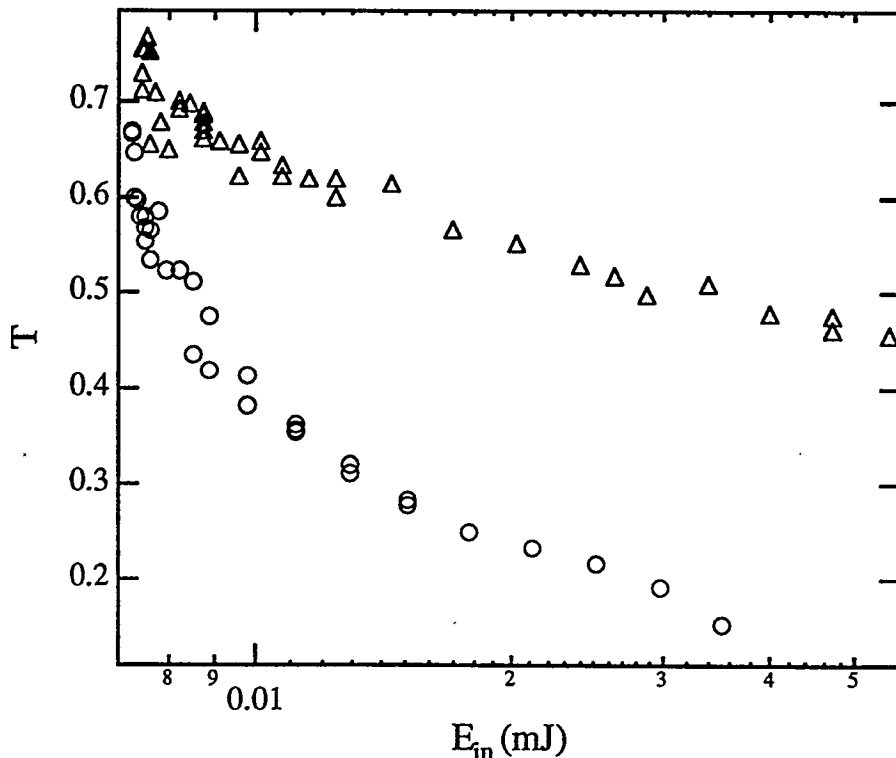


Figure 6. Transmittance vs. incident pulse energy (optical limiting) at 700 nm, for PCBM in o-dichlorobenzene solution (open circles), and in sol-gel glass composite (open triangles). Linear transmittance of both samples is $\approx 70\%$.

Recent analytical and experimental treatments have explored methods to optimize the nonlinear response of RSA materials by incorporating a so-called “bottleneck limiter” geometry, in which the concentration of the active guest is varied along the depth of the focus of a tightly focused laser beam.^{7,8,24-26} The goal of these designs is to increase the dynamic range of existing limiter materials by spreading the nonlinear response over a sample which is large compared to the Rayleigh range (focal depth) of the focused beam, so that at the maximum expected input energy, the internal fluence over the whole sample is nearly constant, and just below the damage fluence of the material. It has been predicted numerically that more than an order of magnitude enhancement in the nonlinear response is possible using these designs, and initial results confirming this enhancement have been reported.^{24,26} Since controlling the concentration in a stepwise fashion is simpler for solid-state samples, and since the damage threshold for the glass composite samples reported in this work is enhanced relative to either solution or PMMA hosts, the sol-gel samples would seem to provide an attractive alternative to traditional approaches for optical limiting, using fullerenes as in this work, or other nonlinear guest molecules. We are currently exploring whether optimizing the concentration profile will allow the design of high damage threshold, solid-state optical limiters which surpass the performance of solution-based systems.

- [12] D. Sheng, R. Compton, J. Young, and G. Mamantov, "Preparation of C₇₀-doped solid silica gel via sol-gel process," *J. Am. Ceram. Soc.* **79**, 2865 (1992).
- [13] M. Maggini, G. Scorrano, M. Prato, G. Brusatin, P. Innocenzi, M. Guglielmi, A. Renier, R. Signorini, M. Meneghetti, and Bozio, R. "C₆₀ derivatives in sol-gel glasses," *Adv. Mater.* **7**, 404 (1995).
- [14] J. C. Hummelen, B. W. Knight, F. Lepec, F. Wudl, J. Yao, and C. L. Wilkins, "Preparation and characterization of fulleroid and methanofullerene derivatives," *J. Org. Chem.* **60**, 532 (1995).
- [15] D. McBranch, L. Smilowitz, V. Klimov, J. Robinson, B. Mattes, A. Koskelo, J. Hummelen, F. Wudl, N. Borrelli, and J. Withers, "Optical limiting in fullerene solutions and doped glasses," *SPIE Proceedings, Fullerenes and Photonics II* **2530**, 195 (1995).
- [16] L. Smilowitz, D. McBranch, V. Klimov, J. Robinson, A. Koskelo, M. Grigorova, B. Mattes, H. Wang, and F. Wudl, "Enhanced optical limiting in derivatized fullerenes," *Opt. Lett.* **21**, 922 (1996).
- [17] R. J. Sension, C. M. Phillips, A. Z. Szarka, W. J. Romanov, A. R. McGhie, J. P. M. Jr., A. B. S. III, and R. M. Hochstrasser, "Transient absorption studies of C₆₀ in solution," *J. Phys. Chem.* **95**, 6075 (1991).
- [18] T. W. Ebbesen, K. Tanigaki, and S. Kuroshima, "Excited-state properties of C₆₀," *Chem. Phys. Lett.* **181**, 501 (1991).
- [19] J. Arbogast, A. Darmanyan, C. Foote, Y. Rubin, F. Diederich, M. Alvarez, S. Anz, and R. Whetten, "Photophysical properties of C₆₀," *J. Phys. Chem.* **95**, 11 (1991).
- [20] B. C. Hess, D. V. Bowersox, S. H. Mardirosian, and L. D. Unterberger, "Electroabsorption in C₆₀ and C₇₀: third-order nonlinearity in molecular and solid states," *Chem. Phys. Lett.* **248**, 141 (1996).
- [21] A. Seilmeyer and W. Kaiser, in *Ultrashort laser pulses: Generation and application*, W. Kaiser, ed., (Springer-Verlag, Berlin 1993).
- [22] S. L. Dexheimer, W. A. Varecka, C. V. Shank, D. Mittelman, and A. Zettl, "Nonexponential relaxation in solid C₆₀ via time-dependent singlet exciton annihilation," *Chem. Phys. Lett.* **235**, 552 (1995).
- [23] A. Kost, L. Tutt, M. Klein, T. Dougherty, and W. Elias, "Optical limiting with C₆₀ in polymethyl methacrylate," *Opt. Lett.* **18**, 334 (1993).
- [24] J. Perry, K. Mansour, P. Miles, C. T. Chen, S. Marder, G. Kwag, and M. Kenney, "Phthalocyanine materials for optical limiting," *Abstr. Am. Chem. Soc.* **209**, 131 (1995).
- [25] T. Xia, D. J. Hagan, A. Dogariu, A. A. Said, and E. W. V. Stryland, "Optimization of optical limiting devices based on excited-state absorption," *Appl. Opt.* in press (1996).
- [26] A. A. Said, T. Xia, D. J. Hagan, A. Wajgrus, S. Yang, D. Kovshi, M. A. Decker, S. Khodja, and E. W. V. Stryland, "Liquid-based multicell optical limiter," *SPIE Proceedings, Nonlinear Optical Liquids* **2853**, in press (1996).

DISCLAIMER

This report was prepared as an account of work sponsored by an agency of the United States Government. Neither the United States Government nor any agency thereof, nor any of their employees, makes any warranty, express or implied, or assumes any legal liability or responsibility for the accuracy, completeness, or usefulness of any information, apparatus, product, or process disclosed, or represents that its use would not infringe privately owned rights. Reference herein to any specific commercial product, process, or service by trade name, trademark, manufacturer, or otherwise does not necessarily constitute or imply its endorsement, recommendation, or favoring by the United States Government or any agency thereof. The views and opinions of authors expressed herein do not necessarily state or reflect those of the United States Government or any agency thereof.